

# Measurements of Relative Branching Ratios of $\Lambda_c^+$ Decays into States Containing $\Sigma$

The FOCUS Collaboration

J. M. Link<sup>a</sup> M. Reyes<sup>a</sup> P. M. Yager<sup>a</sup> J. C. Anjos<sup>b</sup> I. Bediaga<sup>b</sup>  
C. Göbel<sup>b</sup> J. Magnin<sup>b</sup> A. Massafferri<sup>b</sup> J. M. de Miranda<sup>b</sup>  
I. M. Pepe<sup>b</sup> A. C. dos Reis<sup>b</sup> S. Carrillo<sup>c</sup> E. Casimiro<sup>c</sup>  
E. Cuautle<sup>c</sup> A. Sánchez-Hernández<sup>c</sup> C. Uribe<sup>c</sup> F. Vázquez<sup>c</sup>  
L. Agostino<sup>d</sup> L. Cinquini<sup>d</sup> J. P. Cumalat<sup>d</sup> B. O'Reilly<sup>d</sup>  
J. E. Ramirez<sup>d</sup> I. Segoni<sup>d</sup> J. N. Butler<sup>e</sup> H. W. K. Cheung<sup>e</sup>  
G. Chiodini<sup>e</sup> I. Gaines<sup>e</sup> P. H. Garbincius<sup>e</sup> L. A. Garren<sup>e</sup>  
E. Gottschalk<sup>e</sup> P. H. Kasper<sup>e</sup> A. E. Kreymer<sup>e</sup> R. Kutschke<sup>e</sup>  
L. Benussi<sup>f</sup> S. Bianco<sup>f</sup> F. L. Fabbri<sup>f</sup> A. Zallo<sup>f</sup> C. Cawfield<sup>g</sup>  
D. Y. Kim<sup>g</sup> K. S. Park<sup>g</sup> A. Rahimi<sup>g</sup> J. Wiss<sup>g</sup> R. Gardner<sup>h</sup>  
A. Kryemadhi<sup>h</sup> K. H. Chang<sup>i</sup> Y. S. Chung<sup>i</sup> J. S. Kang<sup>i</sup>  
B. R. Ko<sup>i</sup> J. W. Kwak<sup>i</sup> K. B. Lee<sup>i</sup> K. Cho<sup>j</sup> H. Park<sup>j</sup>  
G. Alimonti<sup>k</sup> S. Barberis<sup>k</sup> A. Cerutti<sup>k</sup> M. Boschini<sup>k</sup>  
P. D'Angelo<sup>k</sup> M. DiCorato<sup>k</sup> P. Dini<sup>k</sup> L. Edera<sup>k</sup> S. Erba<sup>k</sup>  
M. Giannarchi<sup>k</sup> P. Inzani<sup>k</sup> F. Leveraro<sup>k</sup> S. Malvezzi<sup>k</sup>  
D. Menasce<sup>k</sup> M. Mezzadri<sup>k</sup> L. Moroni<sup>k</sup> D. Pedrini<sup>k</sup>  
C. Pontoglio<sup>k</sup> F. Prelz<sup>k</sup> M. Rovere<sup>k</sup> S. Sala<sup>k</sup>  
T. F. Davenport III<sup>ℓ</sup> V. Arena<sup>m</sup> G. Boca<sup>m</sup> G. Bonomi<sup>m</sup>  
G. Gianini<sup>m</sup> G. Liguori<sup>m</sup> M. M. Merlo<sup>m</sup> D. Pantea<sup>m</sup>  
S. P. Ratti<sup>m</sup> C. Riccardi<sup>m</sup> P. Vitulo<sup>m</sup> H. Hernandez<sup>n</sup>  
A. M. Lopez<sup>n</sup> H. Mendez<sup>n</sup> L. Mendez<sup>n</sup> E. Montiel<sup>n</sup> D. Olaya<sup>n</sup>  
A. Paris<sup>n</sup> J. Quinones<sup>n</sup> C. Rivera<sup>n</sup> W. Xiong<sup>n</sup> Y. Zhang<sup>n</sup>  
J. R. Wilson<sup>o</sup> T. Handler<sup>p</sup> R. Mitchell<sup>p</sup> D. Engh<sup>q</sup> M. Hosack<sup>q</sup>  
W. E. Johns<sup>q</sup> M. Nehring<sup>q</sup> P. D. Sheldon<sup>q</sup> K. Stenson<sup>q</sup>  
E. W. Vaandering<sup>q</sup> M. Webster<sup>q</sup> M. Sheaff<sup>r</sup>

<sup>a</sup>University of California, Davis, CA 95616

<sup>b</sup>Centro Brasileiro de Pesquisas Físicas, Rio de Janeiro, RJ, Brasil

<sup>c</sup>CINVESTAV, 07000 México City, DF, Mexico

<sup>d</sup>University of Colorado, Boulder, CO 80309

<sup>e</sup>*Fermi National Accelerator Laboratory, Batavia, IL 60510*

<sup>f</sup>*Laboratori Nazionali di Frascati dell'INFN, Frascati, Italy I-00044*

<sup>g</sup>*University of Illinois, Urbana-Champaign, IL 61801*

<sup>h</sup>*Indiana University, Bloomington, IN 47405*

<sup>i</sup>*Korea University, Seoul, Korea 136-701*

<sup>j</sup>*Kyungpook National University, Taegu, Korea 702-701*

<sup>k</sup>*INFN and University of Milano, Milano, Italy*

<sup>l</sup>*University of North Carolina, Asheville, NC 28804*

<sup>m</sup>*Dipartimento di Fisica Nucleare e Teorica and INFN, Pavia, Italy*

<sup>n</sup>*University of Puerto Rico, Mayaguez, PR 00681*

<sup>o</sup>*University of South Carolina, Columbia, SC 29208*

<sup>p</sup>*University of Tennessee, Knoxville, TN 37996*

<sup>q</sup>*Vanderbilt University, Nashville, TN 37235*

<sup>r</sup>*University of Wisconsin, Madison, WI 53706*

---

## Abstract

We have studied the Cabibbo suppressed decay  $\Lambda_c^+ \rightarrow \Sigma^+ K^{*0}(892)$  and the Cabibbo favored decays  $\Lambda_c^+ \rightarrow \Sigma^+ K^+ K^-$ ,  $\Lambda_c^+ \rightarrow \Sigma^+ \phi$  and  $\Lambda_c^+ \rightarrow \Xi^{*0}(\Sigma^+ K^-)K^+$  and measured their branching ratios relative to  $\Lambda_c^+ \rightarrow \Sigma^+ \pi^+ \pi^-$  to be  $(7.8 \pm 1.8 \pm 1.3)\%$ ,  $(7.1 \pm 1.1 \pm 1.1)\%$ ,  $(8.7 \pm 1.6 \pm 0.6)\%$  and  $(2.2 \pm 0.6 \pm 0.6)\%$ , respectively. The first error is statistical and the second is systematic. We also report two 90% confidence level limits  $\Gamma(\Lambda_c^+ \rightarrow \Sigma^- K^+ \pi^+)/\Gamma(\Lambda_c^+ \rightarrow \Sigma^+ K^{*0}(892)) < 35\%$  and  $\Gamma(\Lambda_c^+ \rightarrow \Sigma^+ K^+ K^-)_{NR}/\Gamma(\Lambda_c^+ \rightarrow \Sigma^+ \pi^+ \pi^-) < 2.8\%$ .

---

## 1 Introduction

Past experiments have reported results on non-leptonic branching fractions of the lowest lying charmed baryon  $\Lambda_c^+$  [1,2]. In this paper we report on several  $\Lambda_c^+$  decay channels containing a  $\Sigma$  baryon in the final state. These measurements may be useful in testing theoretical predictions of the contributions to inclusive decay amplitudes. For instance, as pointed out by Guberina and Stefancic [3], direct measurements of  $\Lambda_c^+$  singly Cabibbo suppressed decay rates can improve our theoretical understanding of the  $\Xi_c^+$  lifetime, which can then be compared to recent high statistics measurements [4].

## 2 Reconstruction

This analysis uses data collected by the FOCUS experiment at Fermilab during the 1996-97 fixed-target run and is based on a topological sample of events with a charged Sigma hyperon plus two other charged particles emerging from the  $\Lambda_c^+$  decay vertex.

FOCUS is a photo-production experiment equipped with very precise vertexing and particle identification detectors. The vertexing system is composed of a silicon microstrip detector (TS) [5] interleaved with segments of the BeO target and a second system of twelve microstrip planes (SSD) downstream of the target. Beyond the SSD, five stations of multi-wire proportional chambers plus two large aperture dipole magnets complete the charged particle tracking and momentum measurement system. Three multi-cell, threshold Čerenkov counters discriminate between different particle hypotheses, namely electrons, pions, kaons and protons. The FOCUS apparatus also contains one hadronic and two electromagnetic calorimeters as well as two muon detectors.

Events are selected using a candidate driven vertexing algorithm where the vector components of the reconstructed decay particles define the charm flight direction. This is used as a seed track to find the production vertex [6]. Using this algorithm we determine the confidence level of the decay and production vertices, and the significance of their separation. For each of the decay modes analyzed, we require the primary vertex to have a confidence level greater than 1% and to contain at least two tracks other than the charm seed track.

The  $\Sigma^- \rightarrow n\pi^-$ ,  $\Sigma^+ \rightarrow n\pi^+$  and  $\Sigma^+ \rightarrow p\pi^0$  decays<sup>1</sup> are reconstructed using a kink algorithm [7] where the properties of the neutral particle in the decay are not detected, but rather inferred, with a two-fold ambiguity in the momentum solution for some decays. Systematic effects due to this ambiguity are reduced by normalizing to the decay mode  $\Lambda_c^+ \rightarrow \Sigma^+\pi^+\pi^-$ , where the same effect exists. To aid in fitting the mass distribution, for channels containing a  $\Sigma$ , we implement a double Gaussian to determine the yield of signal events. By double Gaussian we mean two Gaussian shapes with separate amplitudes, means and widths. In this paper we will discuss the  $\Sigma^+\pi^+\pi^-$ ,  $\Sigma^+K^+\pi^-$ ,  $\Sigma^-K^+\pi^+$  and  $\Sigma^+K^+K^-$  final states. In the  $\Lambda_c^+ \rightarrow \Sigma^+\pi^+\pi^-$  mode we let all the parameters float while in the other lower statistics modes we fix some of the parameters to their Monte Carlo values.

---

<sup>1</sup> Throughout this paper the charge conjugate state is implied unless explicitly stated. Note that the  $\Sigma^-$  is not the charge conjugate partner of the  $\Sigma^+$ .

### 3 $\Lambda_c^+ \rightarrow \Sigma^+ \pi^+ \pi^-$ normalization mode

The  $\Lambda_c^+ \rightarrow \Sigma^+ \pi^+ \pi^-$  mode is our highest statistics decay containing a  $\Sigma^+$  particle. The events are selected requiring a detachment between primary and secondary vertex divided by its error ( $l/\sigma_l$ ) greater than 5.5. A minimum  $\Lambda_c^+$  momentum cut of 50 GeV/ $c$  is imposed, as is a minimum secondary vertex confidence level of 10%. We also apply a cut on the lifetime resolution,  $\sigma_t < 120$  fs for the run period where we had a silicon detector (TS) in the target region (about 2/3 of the events) and  $\sigma_t < 150$  fs otherwise (NoTS). Further, we reject events which have a lifetime greater than six times the  $\Lambda_c^+$  lifetime.

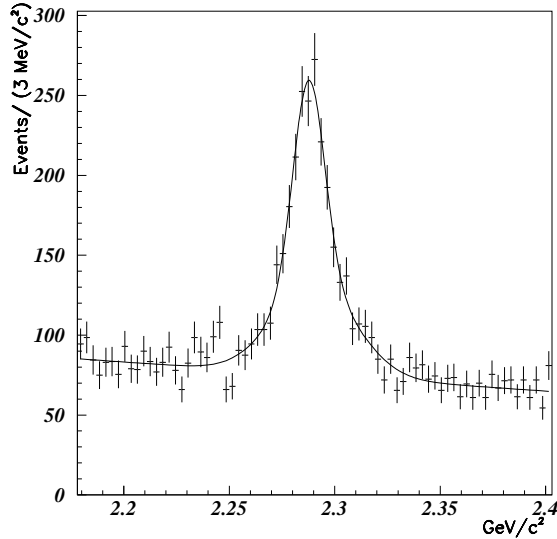


Fig. 1.  $\Sigma^+ \pi^+ \pi^-$  invariant mass distribution fit with a double Gaussian for the signal and a linear background.

We identify charged tracks using information from three Čerenkov counters. The algorithm [8] makes use of the on/off status of the Čerenkov cells to construct a likelihood for the hypothesis that a given track of a certain momentum generates the observed output. Once the likelihood for each hypothesis “ $\alpha$ ” (proton, kaon, pion, electron) has been computed we construct a  $\chi^2$ -like variable  $W_\alpha = -2 \ln(Likelihood_\alpha)$ . We identify particles by comparing these variables.

Our pion consistency (PICON) requirement comes from comparing the minimum  $W_\alpha$  hypothesis to the pion hypothesis. For example, the two pions from  $\Lambda_c^+ \rightarrow \Sigma^+ \pi^+ \pi^-$  decay are required to satisfy PICON= $\min\{W_{\alpha=e,\pi,K,p}\} - W_\pi > -6$ . Further, pions must not be identified as muons by the muon detector. For  $\Sigma^+ \rightarrow p\pi^0$  decays, the proton is required to satisfy  $W_\pi - W_p > -3$  while for  $\Sigma^+ \rightarrow n\pi^+$ , the pion must satisfy  $W_p - W_\pi > -3$  and PICON  $> -6$  and have a momentum greater than 5 GeV/ $c$ .

The  $\Sigma^+\pi^+\pi^-$  mass distribution (Fig. 1) is fit with a double Gaussian and a linear background. We obtain a yield of  $1706 \pm 88$  events.

#### 4 $\Lambda_c^+ \rightarrow \Sigma^+ K^{*0}(892)$ and $\Lambda_c^+ \rightarrow \Sigma^- K^+\pi^+$ decay modes

The  $\Lambda_c^+$  is reconstructed in the decay channel  $\Sigma^+ K^+\pi^-$ . We fit the invariant mass distribution with and without a mass cut ( $832 < M(K\pi) < 960$  MeV/ $c^2$ ) around the  $K^*(892)$  nominal value. We find that most, if not all, of this channel occurs via  $\Sigma^+ K^{*0}(892)$ . The absence of a non-resonant decay may also explain the absence of a signal in the  $\Lambda_c^+$  decay to  $\Sigma^- K^+\pi^+$ . In Fig. 2(a) we show the  $\Sigma^+ K^{*0}$  invariant mass distribution, where the  $K^{*0}$  is reconstructed in the  $K^+\pi^-$  mode. In Fig. 2(b) we plot the  $\Sigma^- K^+\pi^+$  invariant mass distribution where no signal is evident. A possible explanation for the suppression of the non-resonant three body decays may be that no quark pairs need to be created in order to get the  $\Sigma^+ K^{*0}(892)$  state (see Fig. 3).

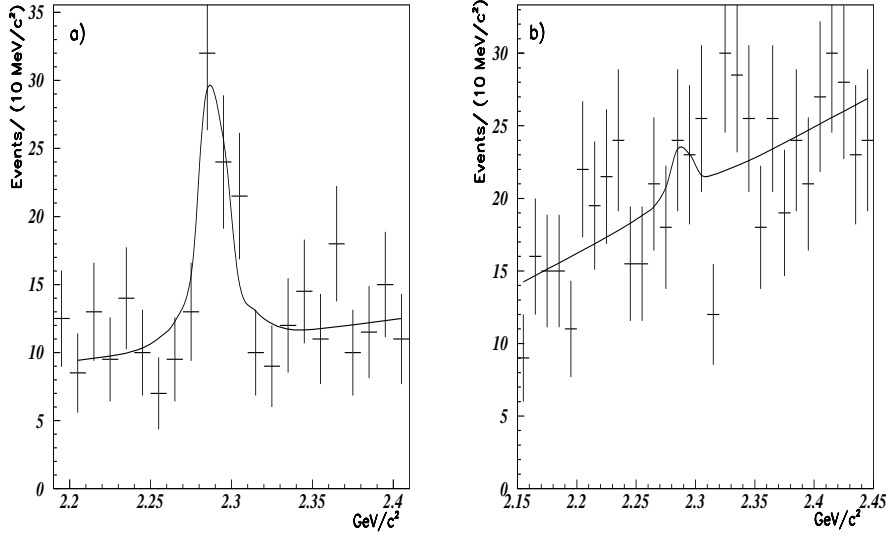


Fig. 2. a) The  $\Sigma^+ K^{*0}$  invariant mass distribution where the  $K^{*0}(892)$  is reconstructed in the  $K^+\pi^-$  channel. Only events in the  $K^*(892)$  signal region are selected. b) Invariant mass distribution for the final state  $\Sigma^- K^+\pi^+$ . The distributions are fit with a double Gaussian for the signal and a linear background.

For the  $\Lambda_c^+ \rightarrow \Sigma^+ K^+\pi^-$  sample we apply a secondary vertex detachment cut,  $l/\sigma_l > 5.5$ , which rejects much of the combinatoric hadronic background. A minimum cut of 50 GeV/ $c$  on the momentum of the  $\Lambda_c^+$  candidate is also applied. The secondary decay vertex must have a confidence level greater than 10%.

Čerenkov identification cuts are applied to the kaon and pion from the  $\Lambda_c^+$

as well as on the charged daughter of the  $\Sigma^+$ . In particular we require  $W_\pi - W_K > 3.5$  on the  $K^+$  while for the pion (from the  $\Lambda_c^+$  decay) we require PICON $> -6$ . In the  $\Sigma^+ \rightarrow p\pi^0$  case we apply a soft pion-proton separation cut of  $W_\pi - W_p > -3$ , while for  $\Sigma^+ \rightarrow n\pi^+$  the pion must satisfy  $W_p - W_\pi > -3$  and PICON $> -6$ . The pion from the  $\Sigma^+$  is also required to have a minimum momentum of  $5 \text{ GeV}/c$ . We remove much of the remaining background by requiring  $\sigma_t < 120 \text{ fs}$  for the TS run period and  $\sigma_t < 150 \text{ fs}$  for the NoTS run period. We also require the lifetime to be less than six times the  $\Lambda_c^+$  lifetime.

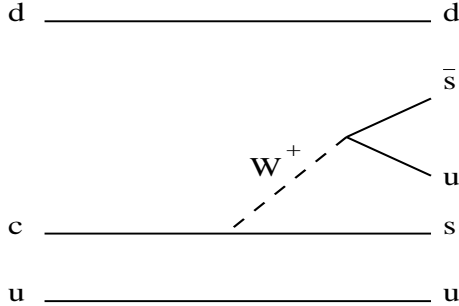


Fig. 3. Spectator diagram for  $\Lambda_c^+ \rightarrow \Sigma^+ K^{*0}(892)$ . In this case no quark pair needs to be created.

The mass distribution is fit using a double Gaussian plus a linear background. We fixed the widths, the relative yield ratio and the shift between the means of the two Gaussians to the Monte Carlo values. The resulting yield is  $49 \pm 10$  events.

Systematic uncertainties were determined by fit variations on binning, fitting range, and counting sideband subtracted events in the  $K^+\pi^-$ -invariant mass distribution. In order to test for possible biases in the fitting procedure, we also performed the fit of the  $\Sigma^+K^+\pi^-$  mass distribution using the Monte Carlo shape. We measured the relative branching ratio for statistically independent sub-samples divided by momentum, particle-antiparticle, run period, and  $\Sigma^+$  decay modes. Using a technique modeled on the PDG S-factor method we evaluated a systematic uncertainty from these split samples. After a correction for the branching ratio of  $K^{*0}(892) \rightarrow K^+\pi^-$ , our final result for the branching ratio of  $\Lambda_c^+ \rightarrow \Sigma^+ K^{*0}(892)$  with respect to  $\Sigma^+\pi^+\pi^-$  is:

$$\frac{\Gamma(\Lambda_c^+ \rightarrow \Sigma^+ K^{*0}(892))}{\Gamma(\Lambda_c^+ \rightarrow \Sigma^+\pi^+\pi^-)} = (7.8 \pm 1.8(\text{stat.}) \pm 1.3(\text{syst.}))\%$$

where the systematic error is obtained by adding in quadrature the contributions from fit variants and split samples.

We searched for the similar Cabibbo suppressed decay channel  $\Lambda_c^+ \rightarrow \Sigma^- K^+\pi^+$ . The event selection is identical to that of the  $\Lambda_c^+ \rightarrow \Sigma^+ K^+\pi^-$  selection where the  $\Sigma^+$  is reconstructed in a neutron and a charged pion. The invariant mass

distribution is shown in Fig. 2. To set an upper limit on the branching ratio for this decay we fit the data using a double Gaussian with a linear background where all the parameters of the Gaussians, except for the total yield, are fixed to the Monte Carlo values. The fit returns a yield of  $10 \pm 11$  events. The systematic uncertainty is computed by varying the range, binning and the fitting shape function. As we do not observe a signal, after correcting by the branching ratio of  $K^{*0}(892) \rightarrow K^+ \pi^-$  we determine an upper limit of:

$$\frac{\Gamma(\Lambda_c^+ \rightarrow \Sigma^- K^+ \pi^+)}{\Gamma(\Lambda_c^+ \rightarrow \Sigma^+ K^{*0}(892))} \leq 35\%$$

with a 90% confidence level, where we have combined the statistical and systematic errors in quadrature.

## 5 $\Lambda_c^+ \rightarrow \Sigma^+ K^+ K^-$ decay mode

The reconstruction of  $\Sigma^+ K^+ K^-$  events requires a detachment cut of  $l/\sigma_l > 3$ , the candidate  $\Lambda_c^+$  must have a minimum momentum of  $30 \text{ GeV}/c$  and a secondary vertex with a minimum confidence level of 1%. The kaons from the  $\Lambda_c^+$  must be favored with respect to the pion hypothesis,  $W_\pi - W_K > 1$ . The identification of the charged pion from the  $\Sigma^+$  (in the  $n\pi^+$  decay mode) is achieved by requiring  $W_p - W_\pi > -3$  and  $\text{PICON} > -6$ . A soft separation cut of  $W_\pi - W_p > -3$ , is applied to the proton for the decay  $\Sigma^+ \rightarrow p\pi^0$ . Further, we require the lifetime resolution  $\sigma_t < 110 \text{ fs}$  for the TS period and  $\sigma_t < 140 \text{ fs}$  for the NoTS period. The invariant mass distribution is plotted in Fig. 4.

We fit the distribution using a double Gaussian for the signal region plus a linear background and find  $103 \pm 15$  events. The widths of the Gaussians, the yield ratio and the shift between the two means are all fixed to Monte Carlo values. Systematic studies were performed in a manner similar to that for the  $\Sigma^+ K^*(892)$  state. Adding in quadrature the two uncertainties obtained by fit variations and split samples we quote the branching ratio for  $\Lambda_c^+ \rightarrow \Sigma^+ K^+ K^-$  relative to  $\Sigma^+ \pi^+ \pi^-$  to be:

$$\frac{\Gamma(\Lambda_c^+ \rightarrow \Sigma^+ K^+ K^-)}{\Gamma(\Lambda_c^+ \rightarrow \Sigma^+ \pi^+ \pi^-)} = (7.1 \pm 1.1(\text{stat.}) \pm 1.1(\text{syst.}))\%.$$

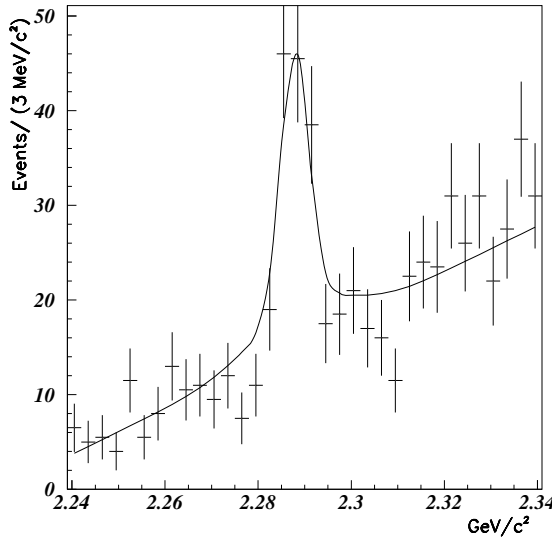


Fig. 4. The fit to the  $\Sigma^+ K^+ K^-$  invariant mass distribution fit with a double Gaussian plus a first degree polynomial.

## 6 $\Lambda_c^+ \rightarrow \Sigma^+ \phi$ decay mode

For the  $\Sigma^+ K^+ K^-$  final state we also measured the resonant  $\Sigma^+ \phi$  contribution. The  $\Sigma^+ \phi$  events are selected using the same cuts used for the  $\Sigma^+ K^+ K^-$  inclusive mode, except: the  $l/\sigma_l$  cut is lowered to 2.5, the  $K^+ K^-$  invariant mass is required to be within  $3\sigma$  ( $10 \text{ MeV}/c^2$ ) of the  $\phi$  mass and the absolute difference between the  $\Sigma^+ K^-$  invariant mass and the  $\Xi^*$  nominal value ( $1.690 \text{ GeV}/c^2$ ) must be greater than  $20 \text{ MeV}/c^2$ . This last cut is applied to suppress the contamination from  $\Lambda_c^+ \rightarrow \Xi^{*0}(1690) K^+$  where the  $\Xi^{*0}$  decays to  $\Sigma^+ K^-$ . A sideband subtraction is performed to remove a possible non-resonant contribution. The  $\Sigma^+ \phi$  invariant mass distribution, with the  $\Xi^{*0}(1690)$  exclusion cut, is shown in Fig. 5.

The fitting procedure follows the strategy applied in the  $\Sigma^+ K^+ K^-$  inclusive mode and give a yield of  $57 \pm 10$  events. To assess the final systematic uncertainty on this measurement, we follow similar criteria to those described previously. We also investigated possible systematic contributions due to our choice of sidebands.

Adding in quadrature the contribution from fit variations and split samples and correcting for the branching fraction of  $\phi$  to  $K^+ K^-$  and the fraction of events lost from our  $\Sigma^+ K^-$  mass cut, we quote the final result for the branching ratio of  $\Lambda_c^+ \rightarrow \Sigma^+ \phi$  with respect to  $\Lambda_c^+ \rightarrow \Sigma^+ \pi^+ \pi^-$  to be :

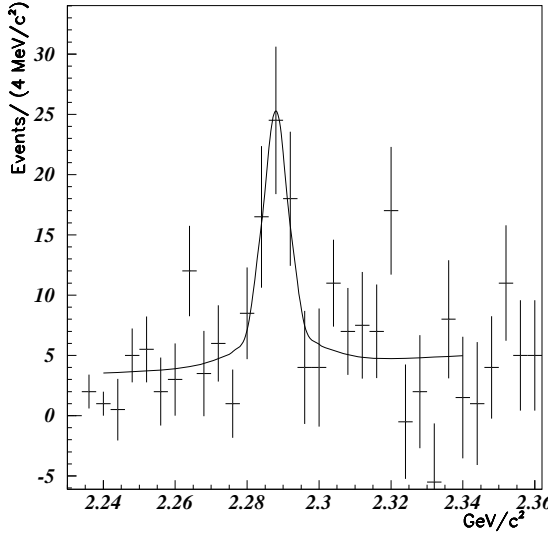


Fig. 5. The figure shows the sideband subtracted invariant mass distribution for  $\Lambda_c^+ \rightarrow \Sigma^+ \phi$  fit using a double Gaussian for the signal and a linear background.

$$\frac{\Gamma(\Lambda_c^+ \rightarrow \Sigma^+ \phi)}{\Gamma(\Lambda_c^+ \rightarrow \Sigma^+ \pi^+ \pi^-)} = (8.7 \pm 1.6(stat.) \pm 0.6(syst.))\%$$

where unseen decay modes of the  $\phi$  are included.

## 7 $\Lambda_c^+ \rightarrow \Xi^{*0}(1690)K^+$ decay mode

We also searched for the decay  $\Lambda_c^+ \rightarrow \Xi^{*0}(1690)K^+$ , with the  $\Xi^{*0}$  reconstructed in  $\Sigma^+ K^-$ . The cuts used in the selection of these events are the same as for the inclusive  $\Sigma^+ K^+ K^-$  mode, except that we lowered the detachment cut to  $l/\sigma_l > 2.5$  and we applied two mass cuts. The first cut excludes the  $\phi$  region by requiring  $M(K^+ K^-) > 1.03 \text{ GeV}/c^2$ . The second cut requires the  $\Sigma^+ K^-$  invariant mass to be within  $20 \text{ MeV}/c^2$  of the  $\Xi^{*0}$  nominal mass of  $1.690 \text{ GeV}/c^2$ . A clean signal is shown in Fig. 6.

We apply the same fitting procedure used in the inclusive decay mode  $\Sigma^+ K^+ K^-$ . The signal yield is  $34 \pm 8$  events. Fit variations and split samples were used to evaluate the systematic uncertainty. We quote a final result of:

$$\frac{\Gamma(\Lambda_c^+ \rightarrow \Xi^{*0}(1690)K^+)}{\Gamma(\Lambda_c^+ \rightarrow \Sigma^+ \pi^+ \pi^-)} * B(\Xi^{*0}(1690) \rightarrow \Sigma^+ K^-) = (2.2 \pm 0.6(stat.) \pm 0.6(syst.))\%.$$

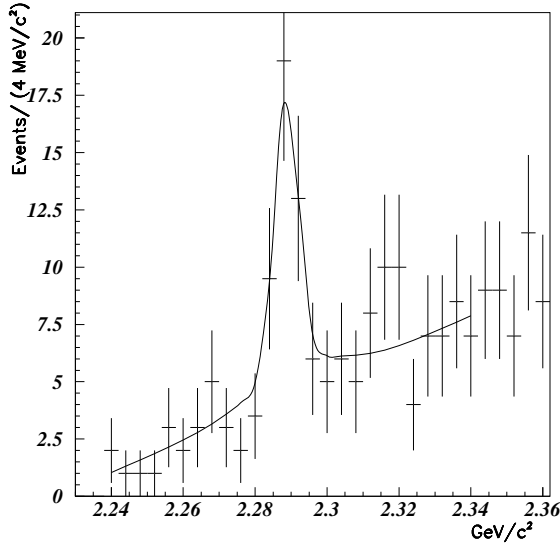


Fig. 6. Invariant mass distribution for the  $\Lambda_c^+$  decay to  $\Xi^{*0}(1690)(\Sigma^+K^-)K^+$  fit with a double Gaussian for the signal and a linear background.

From the measurements of the resonant decays in the  $\Sigma^+K^+K^-$  final state we infer that almost all of  $\Lambda_c^+ \rightarrow \Sigma^+K^+K^-$  occurs through the resonant modes  $\Sigma^+\phi$  and  $\Xi^{*0}(1690)K^+$ .

## 8 Non resonant decay mode $\Lambda_c^+ \rightarrow \Sigma^+K^+K^-$

We also looked for a non-resonant contribution to the decay  $\Lambda_c^+ \rightarrow \Sigma^+K^+K^-$ . We studied the region  $M(K^+K^-) > 1.03$  GeV/ $c^2$  and  $M(\Sigma^+K^-) > 1.71$  GeV/ $c^2$  applying the same selection cuts used in the inclusive mode.

In Fig. 7 we show the  $\Sigma^+K^+K^-$  invariant mass distribution where the double Gaussian fitting procedure has been applied. All the parameters of the double Gaussian, except the total yield, are fixed to their Monte Carlo values. The yield from the fit is  $14 \pm 8$  events. After further corrections due to possible contamination from  $\Lambda_c^+ \rightarrow \Sigma^+\phi$  and  $\Lambda_c^+ \rightarrow \Xi^{*0}(1690)K^+$  decays we find a yield of  $8 \pm 8$  events. With no evidence of a signal, we quote the 90% confidence level limit for the non-resonant component of the decay  $\Lambda_c^+ \rightarrow \Sigma^+K^+K^-$  with respect to  $\Lambda_c^+ \rightarrow \Sigma^+\pi^+\pi^-$  to be:

$$\frac{\Gamma(\Lambda_c^+ \rightarrow \Sigma^+K^+K^-)_{NR}}{\Gamma(\Lambda_c^+ \rightarrow \Sigma^+\pi^+\pi^-)} < 2.5\%.$$

Our systematic error, added in quadrature to the statistical error and included

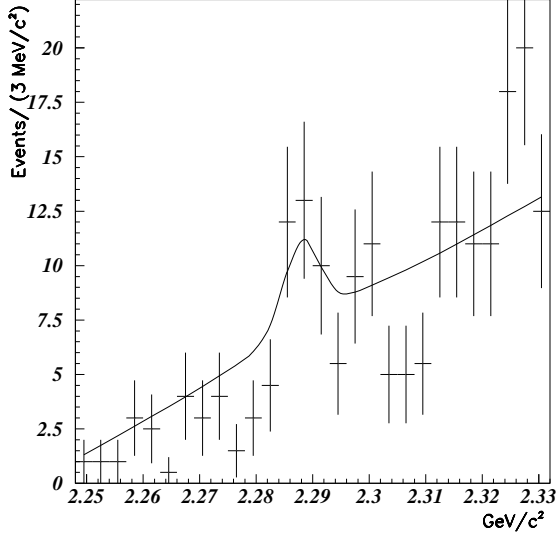


Fig. 7.  $\Lambda_c^+ \rightarrow \Sigma^+ K^+ K^-$  invariant mass distribution for  $M(K^+ K^-) > 1.03$   $\text{GeV}/c^2$  and  $M(\Sigma^+ K^-) > 1.710$   $\text{GeV}/c^2$ . The fit is performed using a double Gaussian for the signal plus a linear background.

in the upper limit, is determined by varying the fit conditions in a manner similar to that previously described.

## 9 Conclusions

Table 1

FOCUS results compared to previous measurements [1,2] where applicable. The relative efficiencies are computed with respect to the normalization mode.

	Efficiency Ratio	FOCUS results	BELLE results	CLEO results
$\frac{\Gamma(\Lambda_c^+ \rightarrow \Sigma^+ K^*(892))}{\Gamma(\Lambda_c^+ \rightarrow \Sigma^+ \pi^+ \pi^-)}$	0.35	$(7.8 \pm 1.8 \pm 1.3)\%$	-	-
$\frac{\Gamma(\Lambda_c^+ \rightarrow \Sigma^- K^+ \pi^+)}{\Gamma(\Lambda_c^+ \rightarrow \Sigma^+ K^*(892))}$	1.49	$< 35\% @ 90\% CL$	-	-
$\frac{\Gamma(\Lambda_c^+ \rightarrow \Sigma^+ K^+ K^-)}{\Gamma(\Lambda_c^+ \rightarrow \Sigma^+ \pi^+ \pi^-)}$	0.85	$(7.1 \pm 1.1 \pm 1.1)\%$	$(7.6 \pm 0.7 \pm 0.9)\%$	$(9.5 \pm 1.7 \pm 1.9)\%$
$\frac{\Gamma(\Lambda_c^+ \rightarrow \Sigma^+ \phi)}{\Gamma(\Lambda_c^+ \rightarrow \Sigma^+ \pi^+ \pi^-)}$	0.39	$(8.7 \pm 1.6 \pm 0.6)\%$	$(8.5 \pm 1.2 \pm 1.2)\%$	$(9.3 \pm 3.2 \pm 2.4)\%$
$\frac{\Gamma(\Lambda_c^+ \rightarrow \Xi^*(\Sigma^+ K^-) K^+)}{\Gamma(\Lambda_c^+ \rightarrow \Sigma^+ \pi^+ \pi^-)}$	0.92	$(2.2 \pm 0.6 \pm 0.6)\%$	$(2.3 \pm 0.5 \pm 0.5)\%$	-
$\frac{\Gamma(\Lambda_c^+ \rightarrow \Sigma^+ K^- K^+)_{NR}}{\Gamma(\Lambda_c^+ \rightarrow \Sigma^+ \pi^+ \pi^-)}$	0.44	$< 2.8\% @ 90\% CL$	$< 1.8\% @ 90\% CL$	-

We have measured the branching ratio of four  $\Lambda_c^+$  decay modes containing a  $\Sigma^+$  particle reconstructed in both the  $p\pi^0$  and  $n\pi^+$  channels. These modes are  $\Lambda_c^+ \rightarrow \Sigma^+ K^{*0}(892)$ ,  $\Lambda_c^+ \rightarrow \Sigma^+ K^+ K^-$  inclusive,  $\Lambda_c^+ \rightarrow \Sigma^+ \phi$  and  $\Lambda_c^+ \rightarrow$

$\Xi^{*0}(\Sigma^+ K^-)K^+$ . For these last two modes our measurements are consistent with the recent results reported by the Belle collaboration [1]. We also set an upper limit for the Cabibbo suppressed decay mode  $\Lambda_c^+ \rightarrow \Sigma^- K^+ \pi^+$  and the non-resonant contribution to  $\Lambda_c^+ \rightarrow \Sigma^+ K^+ K^-$ . Our final results, the relative efficiency of each mode with respect to the normalization mode as well as comparisons to previous measurements, are summarized in Table 1.

## 10 Acknowledgements

We wish to acknowledge the assistance of the staffs of Fermi National Accelerator Laboratory, the INFN of Italy, and the physics departments of the collaborating institutions. This research was supported in part by the U. S. National Science Foundation, the U. S. Department of Energy, the Italian Istituto Nazionale di Fisica Nucleare and Ministero dell’Università e della Ricerca Scientifica e Tecnologica, the Brazilian Conselho Nacional de Desenvolvimento Científico e Tecnológico, CONACyT-México, the Korean Ministry of Education, and the Korean Science and Engineering Foundation.

## References

- [1] K. Abe et al. (Belle), Phys. Lett. B 524 (2002) 33.
- [2] P. Avery et al. (CLEO), Phys. Rev. Lett. 71 (1993) 2391.
- [3] B. Guberina and H. Stefancic (2002), hep-ph/0202080.
- [4] J. M. Link et al. (FOCUS), Phys. Lett. B 523 (2001) 53.
- [5] J. M. Link et al. (FOCUS) (2002), submitted to Nucl. Instrum. Methods A, hep-ex/0204023.
- [6] P. L. Frabetti et al. (E687), Nucl. Instrum. Methods A 320 (1992) 519.
- [7] J. M. Link et al. (FOCUS), Nucl. Instrum. Methods A 484 (2002) 174.
- [8] J. M. Link et al. (FOCUS), Nucl. Instrum. Methods A 484 (2002) 270.